The Role of Protons in and Around Biradicals for Cross-Effect Dynamic Nuclear Polarization

Satyaki Chatterjee,[a] *Amrit Venkatesh,*[b] *Snorri Th. Sigurdsson,*[*a] *Frédéric Mentink-Vigier*[*b]

a. University of Iceland, Department of Chemistry, Science Institute, Dunhaga 3, 107 Reykjavik (Iceland)

b. National High Magnetic Field Laboratory, Florida State University, 1800 E. Paul Dirac Dr, Tallahassee, FL, 32310.

Corresponding Authors

*snorrisi@hi.is, *fmentink@magnet.fsu.edu

ABSTRACT

In magic angle spinning dynamic nuclear polarization, biradicals such as bis-nitroxides are used to hyperpolarize protons under microwave irradiation through the cross-effect mechanism. This mechanism relies on electron-electron spin interactions (dipolar coupling and exchange inter-action) and electron to nuclear spin interactions (hyperfine coupling) to hyperpolarize the protons surrounding the bi-radical. This hyperpolarization is then transferred to the bulk sample via nuclear spin diffusion. However, the involvement of the protons in the biradical in the cross-effect DNP process has been under debate. In this work, we address this question by exploring the hyperpolarization pathways in and around bis-nitroxides. We demonstrate that for biradicals with strong electron-electron interactions, as in the case of the AsymPols, the protons on the biradical may not be necessary to quickly generate hyperpolarization. Instead, such biradicals can efficiently, and directly, polarize the surrounding protons of the solvent. The findings should impact the design of the next generation of biradicals.

TOC GRAPHICS

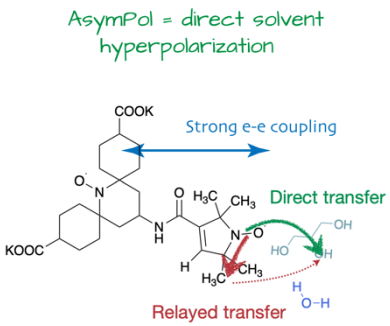

KEYWORDS Dynamic Nuclear Polarization, Spin diffusion barrier, MAS-DNP, electron-electron interactions, NMR, EPR

Solid-state Nuclear Magnetic Resonance (NMR) is one of the most potent way to access atomic-scale information on solids.[1] However, the inherent low sensitivity of solid-state NMR limits its application to investigate low concentrations of NMR active species. This limited sensitivity primarily arises from the low polarization level of the nuclear spins at thermal equilibrium. On the other hand, electron spins have larger spin polarization, due to their higher gyromagnetic ratio ($\gamma_e/\gamma_{1H} \sim 658$). Using the coupling between electron and nearby nuclear spins and using microwave (μw) irradiation at an appropriate frequency, one can increase the nuclear spin polarization through a process called Dynamic Nuclear Polarization (DNP).[2]

In the past decades, DNP has been combined with Magic Angle Spinning (MAS) at high magnetic fields using high-power μw sources, which has enabled the acquisition of MAS NMR

spectra with high resolution and sensitivity.[3–10] DNP has revolutionized the field of solid-state NMR and enabled numerous applications both for biological and material samples,[11–23] in particular at natural isotopic abundance.[24–27]

As of today, MAS-DNP is best carried out using biradicals as polarizing agents,[28,29] that generate high nuclear spin hyperpolarization via a mechanism called cross-effect (CE).[30–33] Biradicals are paramagnetic molecules, with two unpaired electrons spins, that are dissolved in glass-forming matrices such as glycerol/water mixtures and typically used to polarize the protons present in these matrices. The hyperpolarization can be subsequently transferred to the nuclear spins of interest via cross polarization.[34]

The cross-effect DNP mechanism relies on optimal relative g-tensor orientations in the biradical,[32,35–38] strong interelectron spin couplings,[39–44] and sufficiently long electron spin relaxation times. Nuclear hyperpolarization has been improved by preparing bulky molecules,[45–49] and by designing pathways for polarization transfer.[50] Importantly, the cross-effect DNP mechanism relies on the existence of a coupling between the radical centers through space (dipolar coupling, $D_{a,b}$) and through overlap of orbitals (exchange interaction, $J_{a,b}$) – cumulatively these interactions are referred to as e-e couplings, hereafter. In addition, the Electron Paramagnetic Resonance (EPR) spectral width ($\Delta\omega$) of the biradicals must be greater than the Larmor frequency of the protons.

The detailed analysis of cross-effect under MAS has been the subject of several previously reports.[30–33,36,51,52] Briefly, the μw irradiation generates a polarization difference between the two electron spins in the biradical that is transferred to nearby protons. These events occur periodically due to the spinning of the sample and the large breadth of the EPR spectrum, and have been dubbed 'rotor events'.[32] The transfer of the electron spins polarization difference to the proton spins occurs during the cross-effect rotor events. The rate of electron to nucleus polarization transfer involves the e-e couplings, the pseudo-secular hyperfine couplings between electron and proton spins ($A^{\pm}_{a,n}$ and $A^{\pm}_{b,n}$), and the inverse of the Larmor frequency of the nucleus (ω_n).[31,32,53]

Using the Landau-Zener approximation under MAS, the initial rate of the polarization transfer between the biradical and the nuclear spin can be expressed as follows (see Supporting Information for details):

$$R_{\mathrm{CE}} \propto \frac{1}{\Delta\omega_a + \Delta\omega_b} \left| \frac{\left(D_{a,b} + 2J_{a,b}\right)\left(A^{\pm}_{a,n} - A^{\pm}_{b,n}\right)}{\omega_n} \right|^2 \qquad (1)$$

As such, the cross-effect can polarize protons that are close to the electron spins, and the resulting nuclear hyperpolarization is then transferred to protons further way via nuclear spin diffusion.[54] Thus, protons that are close are essential for receiving the hyperpolarization and transmitting the hyperpolarization away from the biradical.

Under standard DNP experimental conditions, proton homonuclear spin diffusion is rapid.[55,56] Indeed, protons far away from the biradical (hereafter referred to as bulk protons) have very similar Larmor frequencies and strong dipolar couplings resulting in an efficient homonuclear spin diffusion. However, the spin diffusion between the protons in the vicinity of the biradical and the ones further away is hindered by the presence of the hyperfine couplings that change their effective Larmor frequency, resulting in a slow transmission of polarization to the bulk protons. The region where these nearby protons with sizeable hyperfine couplings belong to is often referred as the spin diffusion barrier, and its role in the DNP process has been the subject of a long-standing debate.[50,57–60]

In recent years, the role of these nearby protons has been under scrutiny. The advent of numerical models that are able to account for a large number of nuclear spins has highlighted the importance of protons near the biradical.[53,61–63] It has been shown that these nearby protons can periodically exchange their polarization when their Larmor frequency is equal via nuclear dipolar rotor events and thus are essential to the DNP process under MAS.[32,53,63,64]

Recently, the protons on the biradicals have been the center of an extensive study, for example in the case of the bTbK biradical family[35] that possess modest $D_{a,b} \sim 30$ MHz.[61,65] In this comprehensive work, the authors selectively deuterated TEKPol[66] and showed that removing the protons on the molecule lead to a slower hyperpolarization process, i.e. a longer nuclear hyperpolarization time T_B. These observations highlight the importance of strong electron-nuclear hyperfine couplings in the cross-effect rate, in agreement with equation (1).

However, the same equation (1) shows that the initial polarization transfer rate can be modulated by changing the e-e couplings. This rationale was the basis of the design of the AsymPol family of biradicals (

Figure **3**).[40,41] The AsymPols were designed using a conjugated amide linker that enables a close proximity between the two moieties leading to large couplings with $D_{a,b} = 56$ MHz and $J_{a,b} \sim 95$ and 120 MHz (for each of the two conformers).[41] These strong e-e couplings result in increased cross-effect rates and therefore, AsymPol biradicals can generate hyperpolarization very quickly.[40,41] This brings up a simple question: are protons on the biradical as critical in the case of the AsymPols?

In this letter we demonstrate experimentally that, unlike in previous studies,[50,67,68] the protons on the AsymPols are not required for hyperpolarization. We first show that the experimental build-up times are not affected by selective deuteration of AsymPol-COOK, a new derivative of the AsymPols (Figure 1). We then analyze theoretically the process using advanced numerical MAS-DNP simulations. After demonstrating the ability of the numerical methods to predict the build-up times for several complex cases, we then predict the role of the protons on AMUPol[69] and on a AsymPol derivative. We finally discuss how the hyperpolarization is transferred in both cases using a new analytical model and its experimental consequences on the design of new biradicals.

Results - As described above, AsymPols have strong e-e couplings in comparison to TEKPol or AMUPol. This difference is reflected in the initial polarization transfer, which can be indirectly measured by the characteristic time taken to generate bulk hyperpolarization in a radical solution called the build-up time, T_B. It has been demonstrated that the measured build-up time reflects the combined effects of the initial CE polarization rate and the spin diffusion rate (inside and outside of the so-called spin diffusion barrier).[53,57]

We explored the impact of selective deuteration of AsymPol-COOK and its impact on T_B and the DNP enhancements ($\epsilon_{\mathrm{on/off}}$). We carried out the synthesis of AsymPol-COOK as well as AsymPol-COOK-d12 (Figure 1 (a), Scheme S1). AsymPol-COOK is a new water-soluble derivative of AsymPol that is easier to synthesize than AsymPol-POK.[40]

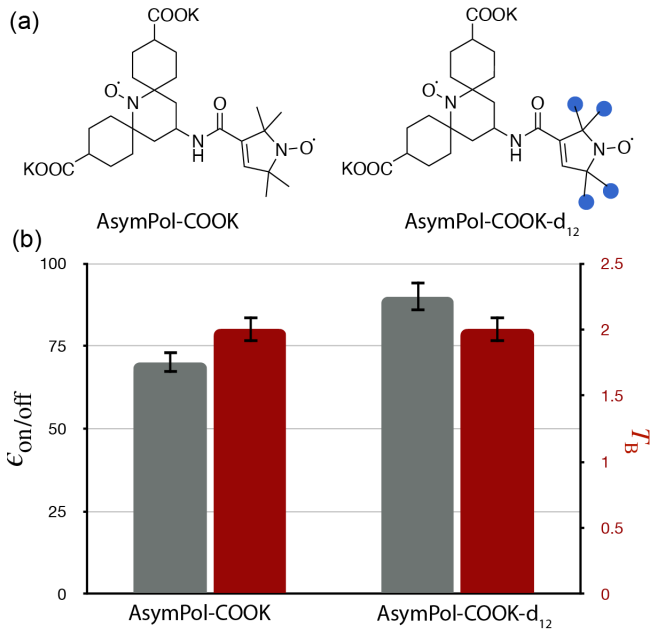

Figure 1: (a) Structures of AsymPol-COOK tested under MAS-DNP at 14.1 T, deuterated sites are indicated in blue. (b) Experimental results: enhancement $\epsilon_{\mathrm{on/off}}$ (grey bars, left axis) and build-up time T_B (red bars, right axis) for 10±0.1 mM of AsymPol-COOK and AsymPol-COOK-d_{12} in glycerol-d_8/D_2O/H_2O (6/3/1 volume ratio).

The MAS-DNP experiments used a 10±1 mM solution of AsymPol-COOK and AsymPol-COOK-d_{12} in a glass forming matrix made of glycerol-d_8/D_2O/H_2O (6/3/1 volume ratio) (see SI for EPR data). The build-up time and enhancement $\epsilon_{\mathrm{on/off}}$ of the two biradicals was measured at 8 kHz and 14.1 T (Figure 1 (b)). The enhancement for the partially deuterated biradical ($\epsilon_{\mathrm{on/off}} = 88 \pm 2$) is higher than for the fully protonated one ($\epsilon_{\mathrm{on/off}} = 68 \pm 2$). This observation is in line with previous works where deuterating the methyl groups in alpha position of the nitroxide group yielded higher enhancements[47,67,68] unlike deuteration of TEKPol.[50] Removal of the protons on the fast relaxing methyl groups has been shown to increase electron spin relaxation times, which likely affects the microwave saturation factor and observed enhancements.[47,67,68] These effects are not completely understood and will be the subject of future work.

Most importantly, the build-up times are identical for both biradicals, $T_B \sim 2 \pm 0.1$ s. This is stark contrast with any previously reported results in which the T_B increased under deuteration.[47,50,67,68] This observation reveals a fundamentally different DNP process for the AsymPols in which the protons on the molecules play a minor role.

To understand the underlying mechanism, we used a previously introduced numerical simulations program of the MAS-DNP process. We first benchmarked our reported model[41,63] to prove it robustly predicts the build-up time under different conditions. This simulation program is used here to simulate the MAS-DNP process with biradical placed at the center of a box made of the matrix in which it is dissolved. This model is suitable to represent how the polarization is transferred from the biradical to the bulk nuclei and thus predict T_B.

Table 1: Evolution of the polarization build-up time, T_B, as a function of the main magnetic field strength for 5 or 10 mM AMUPol in glycerol-d_8/D_2O/H_2O (6/3/1 volume ratio), [^{1}H] = 11 M.

	T_B (s)			
B_0, MAS freq.	exp (10 mM)	sim (10 mM)	exp (5 mM)	sim (5 mM)
9.4 T, 8 kHz	3.5[69]	3.6	7[70]	7.3
9.4 T, 40 kHz	3.8[71]	4.1	7.1[71]	7.7
14.1 T, 8 kHz	4.8[63,69]	4.5	-	8.7
18.8 T, 8 kHz	5[72]	5	15[71]	10.2
18.8 T, 40 kHz[72]	6.6	6.1	18[71]	11.3

The calculations use structures obtained from Molecular Dynamics (MD) simulations as input and describe the MAS-DNP process and the spin diffusion around the biradical, under certain approximations.[41,63] It makes extensive use of the Landau-Zener approximation applied in the Liouville space[53] to ensure a linear scaling of the problem with the number of spins. In addition, the model takes as input the biradical geometry, e-e coupling, and electron to proton interactions. All these parameters can be reasonably obtained from density functional theory (DFT).[41,61,63] We note that both isotropic (Fermi contact) and anisotropic (dipolar) hyperfine couplings are calculated using DFT simulations and are essential to accurately predict the build-up times, as has also been noted previously.[41,50,63] Since this model was developed to simulate simple cases of AMUPol or AsymPol-POK at 10 mM concentration for moderate MAS frequency, and proton concentration [^{1}H] = 11 M,[41,63] we verified its ability to simulate cases beyond its initial focus. It should be noted that the model is able to predict the T_B of AsymPol-POK.[41]

First, the model was tested on the well characterized AMUPol biradical (

Figure **3** (a)). AMUPol is a water soluble bis-nitroxide introduced by Sauvee et *al.*[69] and it possesses relatively strong e-e couplings with $D_{a,b} = 35$ MHz and $J_{a,b} = -15$ MHz.[61,73] Under MAS, $D_{a,b} + 2J_{a,b}$ ranges from –100 to 20 MHz which enables relatively short build-up times on the order of a few seconds. As such AMUPol is an excellent polarizing agent. Table 1 reports T_B as function of the main magnetic field intensity for AMUPol when [^{1}H] = 11 M and different MAS frequencies (8 or 40 kHz). The corresponding simulations shows a good agreement with

the experiments: the magnetic field and MAS frequency trends are clearly reproduced for both biradical concentrations (Table 1). Note that the enhancements were also calculated (SI), but the multi-nuclei model alone is not able to accurately calculate the enhancements, as previously noted.[61,74]

To further test the robustness of the model, T_B was simulated for different proton concentrations and compared with the results recently published by Prisco et al (Figure 2).[57] The excellent agreement between experiments and simulations demonstrates the validity of this multi-nuclei model used in the simulations.

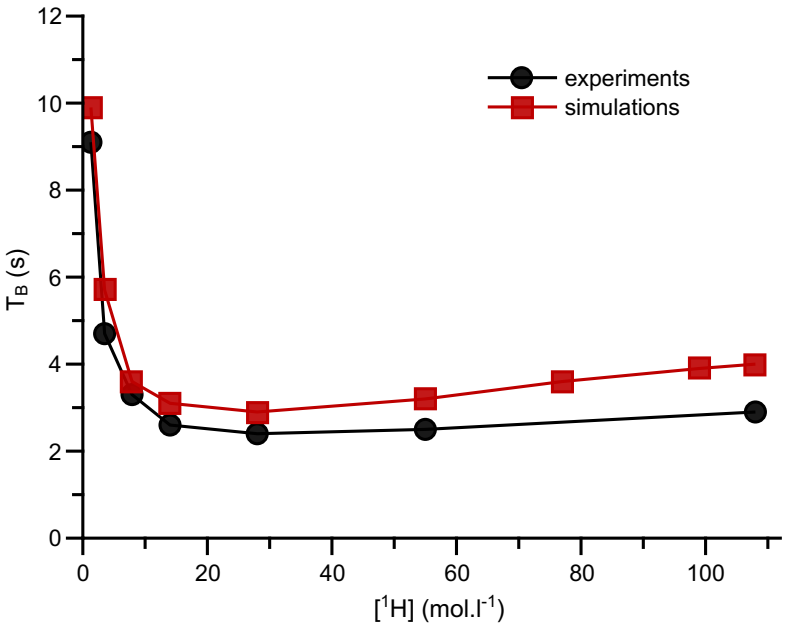

Figure 2: Plot showing T_B as a function of [^{1}H] for 12 mM AMUPol dissolved in mixtures of glycerol/H_2O (6/4 volume ratio) and glycerol-d_8/D_2O (6/4 volume ratio). Black circles, experimental data extracted from ref [57], red squares, simulations.

We subsequently investigated the impact of degree of deuteration of the radicals (Figure **3** (a)) on the DNP build-up times at two different magnetic fields, 9.4 T and 14.1 T (Figure **3** (b)). To simplify the MD simulations, a neutral AsymPol, AsymPol-OH was used for predictions as its geometry is very similar to AsymPol-COOK (see SI).

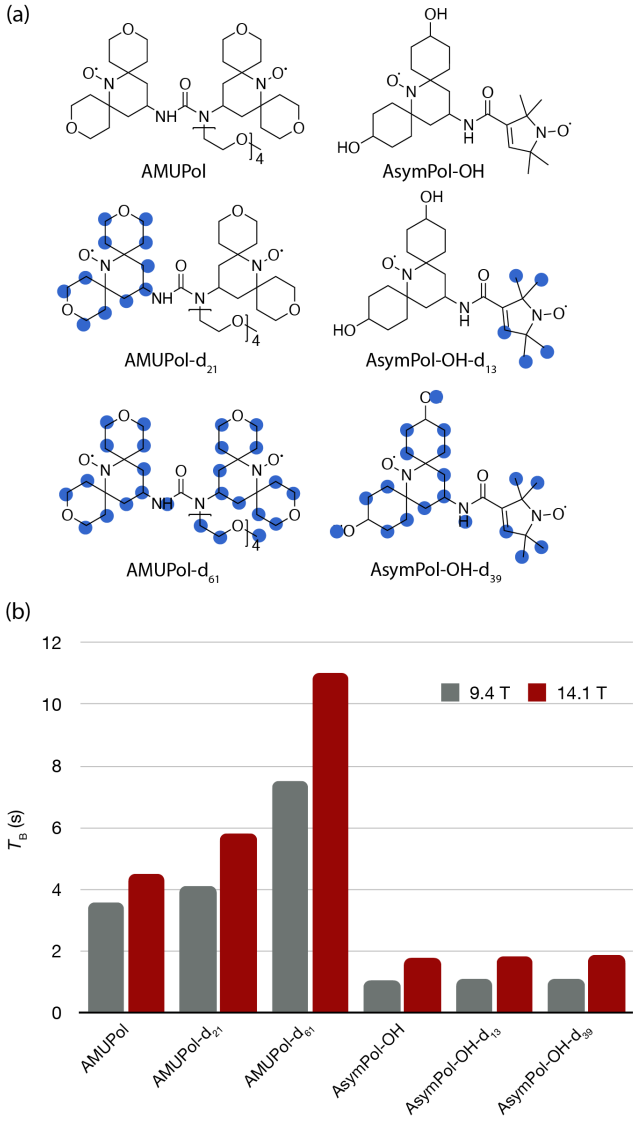

Figure 3: (a) Biradical structures tested for MAS-DNP, deuterated sites are indicated in blue. (b) Calculated build-up times for 10 mM AMUPol or 10 mM AsymPol-OH dissolved in glycerol-d_8/D_2O/H_2O. Three different deuteration levels of the biradicals have been simulated: no deuteration, one radical moiety deuterated, and fully deuterated.

First the non-deuterated biradicals were tested *in silico* (

Figure **3** (b)); AsymPol-OH yields shorter build-up times than AMUPol. At both 9.4 T and 14.1 T, AsymPol-OH was predicted to have build-up times three-fold shorter than AMUPol (1 s vs 3.6 s and 1.8 vs 4.5 s, respectively,

Figure **3** (b)). The simulations were then carried out for the biradicals where only one moiety was deuterated. In that case the build-up time of AMUPol increases to 4.1 s and 5.8 s at 9.4 T and 14.1 T, respectively (

Figure **3** (b)). On the other hand, the build-up times of AsymPol-OH are unaffected by deuteration. When the biradicals are fully deuterated, similar trends are observed: the build-up time of AMUPol becomes significantly longer (7.5 and 11 s at 9.4 T and 14.1 T, respectively), while the build-up time of AsymPol-OH only increases negligibly and remains very close to 1 and 1.8 s at 9.4 and 14.1 T, respectively.

These simulations show differing trends: for AMUPol, the protons on the biradicals are essentials for generating quick nuclear hyperpolarization, while there is no apparent role for these protons in the propagation of hyperpolarization for AsymPol-OH.

Discussion - The hyperpolarization via cross-effect MAS-DNP involves generating an electron spin polarization difference that is transferred to the surrounding nuclei. This process involves the hyperfine couplings and the couplings between the two electron spins in biradicals. Strictly speaking, the efficiency of the polarization transfer depends on the efficiency of the cross-effect rotor events (obtained via the Landau-Zener approximation) and the number of such events per rotor period. These two factors depend on the crystallite

orientation but also depend on the relative orientations of the *g*-tensors.[31,32,36] Since the evolution of the proton polarization is slow compared to the MAS rate,[31,53,62,63] we will ignore the discontinuities induced by the rotor events.

The polarization transfer from the radicals to the bulk nuclei can take two different pathways: (1) polarization of the protons on the molecule followed by spin diffusion to the bulk protons; (2) direct polarization of solvent protons followed by spin diffusion to the bulk protons.

These two pathways can coexist, but their relative contribution may depend on the rate of polarization transfer from the biradicals to each proton (i.e. the cross-effect efficiency), and on the rate of the spin diffusion between protons that are strongly coupled to the electron in the region of the spin diffusion barrier (which depends on the density of protons[50]). The two pathways do not possess the same weight when comparing AMUPol and the AsymPols.

The polarization of the protons in and around the biradical can be approximately described as a set of equations connecting the two pools of protons i.e. those protons that are on the biradical (N_{birad}), and those that are in the solvent N_{solv}:

$$\begin{aligned}\frac{dP_{\mathrm{birad}}}{dt} &= -R_{\mathrm{CE}}^{\mathrm{birad}}(P_{\mathrm{birad}} - \Delta P_e) - R_{1,n}^{\mathrm{birad}}(P_{\mathrm{birad}} - P_B) - R_{\mathrm{SD}}(\mathrm{P}_{\mathrm{birad}} - \mathrm{P}_{\mathrm{solv}}) \\ \frac{dP_{\mathrm{solv}}}{dt} &= -R_{\mathrm{CE}}^{\mathrm{solv}}(P_{\mathrm{solv}} - \Delta P_e) - R_{1,n}^{\mathrm{solv}}(P_{\mathrm{solv}} - P_B) \\ &\quad - R_{\mathrm{SD}} N_{\mathrm{birad}}/N_{\mathrm{solv}}(\mathrm{P}_{\mathrm{solv}} - \mathrm{P}_{\mathrm{birad}}),\end{aligned} \tag{2}$$

where $R_{\mathrm{CE}}^{\mathrm{birad}}$ and $R_{\mathrm{CE}}^{\mathrm{solv}}$ is the average R_{CE} for the protons on the biradicals and in the solvent, respectively, $R_{1,n}^{\mathrm{birad}}$ and $R_{1,n}^{\mathrm{solv}}$ are the nuclear relaxation rate for the protons on the biradicals

and in the solvent, respectively, R_{SD} is the spin diffusion or exchange rate between the two pools of protons, P_B is the thermal equilibrium polarization, P_{birad} and P_{solv} are polarization levels of the protons on the biradical molecule and solvent matrix, respectively, and ΔP_e is the absolute value of the polarization difference between the electron spins at steady state.[32,36]

If we assume that differences in the proton distribution around both biradicals are negligible, which results in similar magnitude of hyperfine couplings, then R_{SD}, and $A^{\pm}$ are identical. Furthermore, we assume that the EPR linewidths are also similar for both biradicals ($\Delta\omega_{\text{Asym}} \approx \Delta\omega_{\text{AMU}}$), this implies that the ratio

$$\frac{R_{CE}^{\text{birad}}(\text{AsymPol})}{R_{CE}^{\text{birad}}(\text{AMUPol})} = \frac{R_{CE}^{\text{solv}}(\text{AsymPol})}{R_{CE}^{\text{solv}}(\text{AMUPol})} = \frac{|D_{\text{Asym}}+2J_{\text{Asym}}|^2}{|D_{\text{AMU}}+2J_{\text{AMU}}|^2}, \quad (3)$$

mainly depends on ratio of the strength of the e-e couplings of both biradicals. For AMUPol $|D_{\text{AMU}} + 2J_{\text{AMU}}|$ spans the range of 20-100 MHz, while in the case of AsymPols $|D_{\text{Asym}} + 2J_{\text{Asym}}|$ spans a range of 120-300 MHz. Therefore, the AsymPols can hyperpolarize protons faster due to larger R_{CE} by a factor $(120/20)^2$-$(300/100)^2$~ 9-36 on average than AMUPol.

A consequence of this much stronger R_{CE}, AsymPol can achieve the same polarization rate as AMUPol on protons that have hyperfine couplings that are 3-6 times smaller, i.e located at $\approx 3^{\frac{1}{3}}$ -$6^{\frac{1}{3}}$ $\approx$ 1.5 to 2 times further away we assume all other parameters constant. Therefore, AsymPol can more easily hyperpolarize protons in the solvent and does not require the protons on the biradical as predicted by simulations.

Since the polarization build-up time of AsymPol is unchanged, $T_B \approx 1.8$ s, this means that the transfer rate $R_{\mathrm{SD}} \frac{N_{\mathrm{birad}}}{N_{\mathrm{solv}}}$ between the protons of biradical and those of the solvent can be neglected compared to $R_{\mathrm{CE}}^{\mathrm{solv}}$(AsymPol). Therefore, the equations become decoupled:

$$\begin{aligned} \frac{dP_{\mathrm{Asym}}}{dt} &= -R_{\mathrm{CE}}^{\mathrm{Asym}}\left(P_{\mathrm{Asym}} - \Delta P_e^{\mathrm{Asym}}\right) - R_{1,n}^{\mathrm{Asym}}\left(P_{\mathrm{Asym}} - P_B\right) \\ \frac{dP_{\mathrm{solv}}}{dt} &= -R_{\mathrm{CE}}^{\mathrm{solv}}\left(P_{\mathrm{solv}} - \Delta P_e^{\mathrm{Asym}}\right) - R_{1,n}^{\mathrm{solv}}(P_{\mathrm{solv}} - P_B) \end{aligned} \tag{4}$$

In contrast, the large change for T_B in AMUPol vs AMUPol-d$_{21}$, from 4.5 to 5.8 s, means that $R_{\mathrm{CE}}^{\mathrm{solv}}(\mathrm{AMUPol}) < R_{\mathrm{SD}}$. For AMUPol the equation then becomes:

$$\begin{aligned} \frac{dP_{\mathrm{AMU}}}{dt} &= -R_{\mathrm{CE}}^{\mathrm{AMU}}(P_{\mathrm{AMU}} - \Delta P_e^{\mathrm{AMU}}) \\ &- R_{1,n}^{\mathrm{AMU}}(P_{\mathrm{AMU}} - P_B) - R_{\mathrm{SD}}(\mathrm{P}_{\mathrm{AMU}} - P_{\mathrm{solv}}) \\ \frac{dP_{\mathrm{solv}}}{dt} &= -r_{1,n}^{\mathrm{solv}}(P_{\mathrm{solv}} - P_B) - \frac{R_{\mathrm{SD}} N_{\mathrm{birad}}}{N_{\mathrm{solv}}}(P_{\mathrm{solv}} - \mathrm{P}_{\mathrm{AMU}}) \end{aligned} \tag{5}$$

Using the appropriate order of magnitude for those quantities in the equation, this simple model can reproduce the simulated trends as discussed in the SI. However, the simple rate equation model is not quantitative, and thus cannot substitute the multi-nuclei model used to perform calculations above.

The preferred polarization pathways for AMUPol and AsymPol at 14.1 T are shown schematically in Figure 4. As R_{CE} diminishes with field due to the combined effect of $\Delta\omega_a + \Delta\omega_b$ and ω_n^2 in equation (1) the build-up times tends to be longer at high fields.[71] Under very

high field conditions, the protons on the biradicals may once again be important for the AsymPols. In addition, MAS-DNP simulations for larger solvent proton concentration (66 M), show that in that case the protons in the solvent can play a more prominent role. The effect of biradical deuteration remains important but, due to the larger [^{1}H], the protons around the biradical play a more a active part in the hyperpolarization process (see SI).

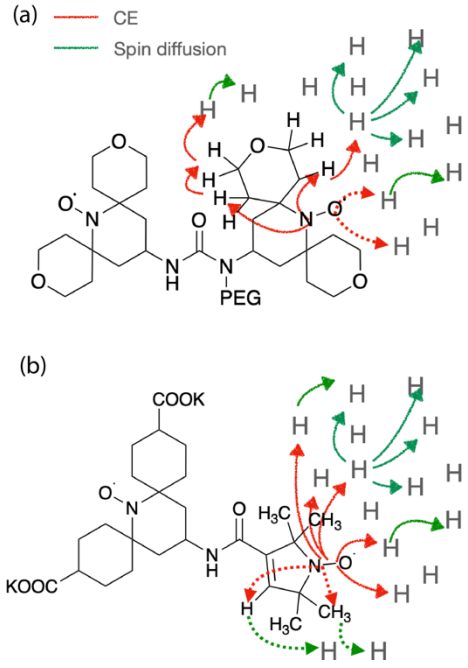

Figure 4: Hyperpolarization pathways for (a) AMUPol and (b) AsymPol-COOK. Red arrows indicate direct polarization transfer via CE, and green arrows indicate proton homonuclear spin diffusion. Full line corresponds to the preferred pathway while dotted lines corresponds to the less favorable one.

We note that in the previous work on the series of deuterated TEKPols,[50] the cross-effect rate is likely limited by relatively low e-e couplings in comparison to the AsymPols. Consequently, the dominant pathway is the hyperpolarization of the closest spins on the biradical molecule. Analogous arguments are also valid for the observations made by Oschkinat and co-workers in the case of TOTAPOL.[67]

Finally, an increase in R_{CE} is desirable but increasing the e-e coupling may not be the only solution. Indeed a large e-e coupling can favor electron-electron cross-relaxation that prevents the generation of large ΔP_e [32] and if larger than $|\omega_n|$ the CE rotor events disappear.[42,44] It is possible that the presence of electron-electron cross-relaxation limits the performance of the AsymPols and other biradicals with large e-e couplings.[42,44]

Instead an increase in R_{CE} can equivalently be achieved by using biradicals with correct relative orientations (which increases the number of CE rotor events),[36] or by using hetero-biradicals,[42,75,76] i.e. molecules made of two different radical types with different EPR linewidth. The latter impacts $\Delta\omega_a + \Delta\omega_b$ in equation (1).

Conclusions - In this work we have studied the hyperpolarization pathways around AsymPol-COOK, a new water-soluble derivative of the AsymPol family. The experiments showed that the build-up time is unaffected by selective deuteration, unlike previous studies.[50,67,68] To understand the underlying mechanism, numerical simulations were performed on two commonly used families of biradicals for MAS-DNP experiments, AMUPol and the

AsymPols. After demonstrating that the MAS-DNP simulations can reproduce the experimental build-up times of AMUPol under numerous conditions, we predicted the effect of biradical deuteration using AMUPol and AsymPol-OH as models. The simulations revealed that T_B for AsymPols do not change under any of the deuteration levels tested. This contrasts with previous reports, notably on the bTbK family[35,50] and indicates a different pathway for the hyperpolarization around the AsymPol confirming the experiments.

These results show that protons near the radical centers of biradicals with moderate e-e coupling, play a significant role in the hyperpolarization pathways. Another highlight of this work is that the so-called diffusion barrier is rather permissible in the case of MAS-DNP: in this region the hyperpolarization transfer is slowed down, but not quenched as the term "barrier" might imply.

Taken together, our results not only reveal the intricacies of the hyperpolarization mechanism, but also demonstrate that when the e-e couplings are large, protons on the biradical are not necessary. Next generation of biradicals should thus focus on increasing the e-e interaction but also improve the relative g-tensor orientation or build on the potential of hetero-biradicals. This will favor an efficient polarization transfer even in difficult media, i.e. fully protonated media,[41,57] but also cases where the targeted nuclear spin is low concentration or is not present on the biradical, e.g. ^{19}F. We note that a similar conclusion has been reached in a recent preprint.[77]

ASSOCIATED CONTENT

Simulations parameters and experimental conditions are available in the Supporting Information

The following files are available free of charge.

Supporting information: 2023-12-11_Fred-Mentink_SpinDiff_SI.pdf

AUTHOR INFORMATION

Corresponding Authors

Snorri Th. Sigurdsson: University of Iceland, Department of Chemistry, Science Institute, Dunhaga 3, 107 Reykjavik (Iceland). ORCID: 0000-0003-2492-1456, Email: snorrisi@hi.is

Frédéric Mentink-Vigier: National High Magnetic Field Laboratory, Florida State University, 1800 E. Paul Dirac Dr, Tallahassee, FL, 32310, ORCID: 0000-0002-3570-9787, Email: fmentink@magnet.fsu.edu

Authors

Satyaki Chatterjee: University of Iceland, Department of Chemistry, Science Institute, Dunhaga 3, 107 Reykjavik (Iceland).

Amrit Venkatesh: National High Magnetic Field Laboratory, Florida State University, 1800 E. Paul Dirac Dr, Tallahassee, FL, 32310.

The authors declare no competing financial interests.

ACKNOWLEDGMENTS

The National High Magnetic Field laboratory (NHMFL) is funded by the National Science Foundation Division of Materials Research (DMR-1644779 and DMR-2128556) and the State of Florida. A portion of this work was supported by the NIH P41 GM122698 and RM1-GM148766. This project has received partial support from the European Union's Horizon 2020 research and innovation programme under Grant Agreement No 101008500 (PANACEA).

This work was supported by the Icelandic Research Fund, grant No. 239662, the University of Iceland Research Fund (S.Th.S) and a doctoral fellowship from the University of Iceland Research Fund (SC).

REFERENCES

(1) Reif, B.; Ashbrook, S. E.; Emsley, L.; Hong, M. Solid-State NMR Spectroscopy. *Nat Rev Methods Primers* **2021**, *1* (1), 1–23. https://doi.org/10.1038/s43586-020-00002-1.

(2) Overhauser, A. W. Polarization of Nuclei in Metals. *Phys. Rev.* **1953**, *92* (2), 411–415. https://doi.org/10.1103/PhysRev.92.411.

(3) Barnes, A. B.; De Paëpe, G.; van der Wel, P. C. A.; Hu, K.-N.; Joo, C.-G.; Bajaj, V. S.; Mak-Jurkauskas, M. L.; Sirigiri, J. R.; Herzfeld, J.; Temkin, R. J.; Griffin, R. G. High-Field Dynamic Nuclear Polarization for Solid and Solution Biological NMR. *Appl Magn Reson* **2008**, *34* (3–4), 237–263. https://doi.org/10.1007/s00723-008-0129-1.

(4) Rosay, M.; Blank, M.; Engelke, F. Instrumentation for Solid-State Dynamic Nuclear Polarization with Magic Angle Spinning NMR. *Journal of Magnetic Resonance* **2016**, *264*, 88–98. https://doi.org/10.1016/j.jmr.2015.12.026.

(5) Biedenbänder, T.; Aladin, V.; Saeidpour, S.; Corzilius, B. Dynamic Nuclear Polarization for Sensitivity Enhancement in Biomolecular Solid-State NMR. *Chem. Rev.* **2022**, *122* (10), 9738–9794. https://doi.org/10.1021/acs.chemrev.1c00776.
(6) Chow, W. Y.; De Paëpe, G.; Hediger, S. Biomolecular and Biological Applications of Solid-State NMR with Dynamic Nuclear Polarization Enhancement. *Chem. Rev.* **2022**, *122* (10), 9795–9847. https://doi.org/10.1021/acs.chemrev.1c01043.
(7) Ghassemi, N.; Poulhazan, A.; Deligey, F.; Mentink-Vigier, F.; Marcotte, I.; Wang, T. Solid-State NMR Investigations of Extracellular Matrixes and Cell Walls of Algae, Bacteria, Fungi, and Plants. *Chem. Rev.* **2022**, *122* (10), 10036–10086. https://doi.org/10.1021/acs.chemrev.1c00669.
(8) Rossini, A. J.; Zagdoun, A.; Lelli, M.; Lesage, A.; Copéret, C.; Emsley, L. Dynamic Nuclear Polarization Surface Enhanced NMR Spectroscopy. *Acc. Chem. Res.* **2013**, *46* (9), 1942–1951. https://doi.org/10.1021/ar300322x.
(9) Rankin, A. G. M.; Trébosc, J.; Pourpoint, F.; Amoureux, J.-P.; Lafon, O. Recent Developments in MAS DNP-NMR of Materials. *Solid State Nuclear Magnetic Resonance* **2019**, *101*, 116–143. https://doi.org/10.1016/j.ssnmr.2019.05.009.
(10) Lilly Thankamony, A. S.; Wittmann, J. J.; Kaushik, M.; Corzilius, B. Dynamic Nuclear Polarization for Sensitivity Enhancement in Modern Solid-State NMR. *Progress in Nuclear Magnetic Resonance Spectroscopy* **2017**, *102–103*, 120–195. https://doi.org/10.1016/j.pnmrs.2017.06.002.
(11) Venkatesh, A.; Lund, A.; Rochlitz, L.; Jabbour, R.; Gordon, C. P.; Menzildjian, G.; Viger-Gravel, J.; Berruyer, P.; Gajan, D.; Copéret, C.; Lesage, A.; Rossini, A. J. The Structure of Molecular and Surface Platinum Sites Determined by DNP-SENS and Fast MAS 195Pt Solid-State NMR Spectroscopy. *J. Am. Chem. Soc.* **2020**, *142* (44), 18936–18945. https://doi.org/10.1021/jacs.0c09101.
(12) Liao, W.-C.; Ghaffari, B.; Gordon, C. P.; Xu, J.; Copéret, C. Dynamic Nuclear Polarization Surface Enhanced NMR Spectroscopy (DNP SENS): Principles, Protocols, and Practice. *Current Opinion in Colloid & Interface Science* **2018**, *33*, 63–71. https://doi.org/10.1016/j.cocis.2018.02.006.
(13) Deligey, F.; Frank, M. A.; Cho, S. H.; Kirui, A.; Mentink-Vigier, F.; Swulius, M. T.; Nixon, B. T.; Wang, T. Structure of *In Vitro* -Synthesized Cellulose Fibrils Viewed by Cryo-Electron Tomography and ^{13} C Natural-Abundance Dynamic Nuclear Polarization Solid-State NMR. *Biomacromolecules* **2022**, *23* (6), 2290–2301. https://doi.org/10.1021/acs.biomac.1c01674.
(14) Lafon, O.; Rosay, M.; Aussenac, F.; Lu, X.; Trébosc, J.; Cristini, O.; Kinowski, C.; Touati, N.; Vezin, H.; Amoureux, J.-P. Beyond the Silica Surface by Direct Silicon-29 Dynamic Nuclear Polarization. *Angew. Chem. Int. Ed.* **2011**, *50* (36), 8367–8370. https://doi.org/10.1002/anie.201101841.
(15) Lesage, A.; Lelli, M.; Gajan, D.; Caporini, M. A.; Vitzthum, V.; Miéville, P.; Alauzun, J.; Roussey, A.; Thieuleux, C.; Mehdi, A.; Bodenhausen, G.; Coperet, C.; Emsley, L. Surface

Enhanced NMR Spectroscopy by Dynamic Nuclear Polarization. *J. Am. Chem. Soc.* **2010**, *132* (44), 15459–15461. https://doi.org/10.1021/ja104771z.

(16) Lee, D.; Duong, N. T.; Lafon, O.; De Paëpe, G. Primostrato Solid-State NMR Enhanced by Dynamic Nuclear Polarization: Pentacoordinated Al $^{3+}$ Ions Are Only Located at the Surface of Hydrated γ-Alumina. *J. Phys. Chem. C* **2014**, *118* (43), 25065–25076. https://doi.org/10.1021/jp508009x.

(17) Rossini, A. J.; Zagdoun, A.; Lelli, M.; Canivet, J.; Aguado, S.; Ouari, O.; Tordo, P.; Rosay, M.; Maas, W. E.; Copéret, C.; Farrusseng, D.; Emsley, L.; Lesage, A. Dynamic Nuclear Polarization Enhanced Solid-State NMR Spectroscopy of Functionalized Metal-Organic Frameworks. *Angew. Chem. Int. Ed.* **2012**, *51* (1), 123–127. https://doi.org/10.1002/anie.201106030.

(18) Chen, Y.; Dorn, R. W.; Hanrahan, M. P.; Wei, L.; Blome-Fernández, R.; Medina-Gonzalez, A. M.; Adamson, M. A. S.; Flintgruber, A. H.; Vela, J.; Rossini, A. J. Revealing the Surface Structure of CdSe Nanocrystals by Dynamic Nuclear Polarization-Enhanced ^{77} Se and ^{113} Cd Solid-State NMR Spectroscopy. *J. Am. Chem. Soc.* **2021**, *143* (23), 8747–8760. https://doi.org/10.1021/jacs.1c03162.

(19) Lee, D.; Leroy, C.; Crevant, C.; Bonhomme-Coury, L.; Babonneau, F.; Laurencin, D.; Bonhomme, C.; De Paëpe, G. Interfacial Ca2+ Environments in Nanocrystalline Apatites Revealed by Dynamic Nuclear Polarization Enhanced 43Ca NMR Spectroscopy. *Nat Commun* **2017**, *8* (1), 14104. https://doi.org/10.1038/ncomms14104.

(20) Chow, W. Y.; Li, R.; Goldberga, I.; Reid, D. G.; Rajan, R.; Clark, J.; Oschkinat, H.; Duer, M. J.; Hayward, R.; Shanahan, C. M. Essential but Sparse Collagen Hydroxylysyl Post-Translational Modifications Detected by DNP NMR. *Chem. Commun.* **2018**, *54* (89), 12570–12573. https://doi.org/10.1039/C8CC04960B.

(21) Jaudzems, K.; Polenova, T.; Pintacuda, G.; Oschkinat, H.; Lesage, A. DNP NMR of Biomolecular Assemblies. *Journal of Structural Biology* **2019**, *206* (1), 90–98. https://doi.org/10.1016/j.jsb.2018.09.011.

(22) Frederick, K. K.; Michaelis, V. K.; Corzilius, B.; Ong, T.-C.; Jacavone, A. C.; Griffin, R. G.; Lindquist, S. Sensitivity-Enhanced NMR Reveals Alterations in Protein Structure by Cellular Milieus. *Cell* **2015**, *163* (3), 620–628. https://doi.org/10.1016/j.cell.2015.09.024.

(23) Smith, A. N.; Märker, K.; Piretra, T.; Boatz, J. C.; Matlahov, I.; Kodali, R.; Hediger, S.; van der Wel, P. C. A.; De Paëpe, G. Structural Fingerprinting of Protein Aggregates by Dynamic Nuclear Polarization-Enhanced Solid-State NMR at Natural Isotopic Abundance. *J. Am. Chem. Soc.* **2018**, *140* (44), 14576–14580. https://doi.org/10.1021/jacs.8b09002.

(24) Perras, F. A.; Kobayashi, T.; Pruski, M. Natural Abundance 17O DNP Two-Dimensional and Surface-Enhanced NMR Spectroscopy. *J. Am. Chem. Soc.* **2015**, *137* (26), 8336–8339. https://doi.org/10.1021/jacs.5b03905.

(25) Märker, K.; Paul, S.; Fernández-de-Alba, C.; Lee, D.; Mouesca, J.-M.; Hediger, S.; De Paëpe, G. Welcoming Natural Isotopic Abundance in Solid-State NMR: Probing π-

Stacking and Supramolecular Structure of Organic Nanoassemblies Using DNP. *Chem. Sci.* **2017**, *8* (2), 974–987. https://doi.org/10.1039/C6SC02709A.

(26) Takahashi, H.; Lee, D.; Dubois, L.; Bardet, M.; Hediger, S.; De Paëpe, G. Rapid Natural-Abundance 2D ^{13}C-^{13}C Correlation Spectroscopy Using Dynamic Nuclear Polarization Enhanced Solid-State NMR and Matrix-Free Sample Preparation. *Angew. Chem. Int. Ed.* **2012**, *51* (47), 11766–11769. https://doi.org/10.1002/anie.201206102.

(27) Hanrahan, M. P.; Chen, Y.; Blome-Fernández, R.; Stein, J. L.; Pach, G. F.; Adamson, M. A. S.; Neale, N. R.; Cossairt, B. M.; Vela, J.; Rossini, A. J. Probing the Surface Structure of Semiconductor Nanoparticles by DNP SENS with Dielectric Support Materials. *J. Am. Chem. Soc.* **2019**, *141* (39), 15532–15546. https://doi.org/10.1021/jacs.9b05509.

(28) Hu, K.-N.; Yu, H.; Swager, T. M.; Griffin, R. G. Dynamic Nuclear Polarization with Biradicals. *J. Am. Chem. Soc.* **2004**, *126* (35), 10844–10845. https://doi.org/10.1021/ja039749a.

(29) Casano, G.; Karoui, H.; Ouari, O. Polarizing Agents: Evolution and Outlook in Free Radical Development for DNP. **2018**, *7*. https://doi.org/10.1002/9780470034590.emrstm1547.

(30) Mentink-Vigier, F.; Akbey, Ü.; Hovav, Y.; Vega, S.; Oschkinat, H.; Feintuch, A. Fast Passage Dynamic Nuclear Polarization on Rotating Solids. *Journal of Magnetic Resonance* **2012**, *224*, 13–21. https://doi.org/10.1016/j.jmr.2012.08.013.

(31) Thurber, K. R.; Tycko, R. Theory for Cross Effect Dynamic Nuclear Polarization under Magic-Angle Spinning in Solid State Nuclear Magnetic Resonance: The Importance of Level Crossings. *The Journal of Chemical Physics* **2012**, *137* (8), 084508. https://doi.org/10.1063/1.4747449.

(32) Mentink-Vigier, F.; Akbey, Ü.; Oschkinat, H.; Vega, S.; Feintuch, A. Theoretical Aspects of Magic Angle Spinning - Dynamic Nuclear Polarization. *Journal of Magnetic Resonance* **2015**, *258*, 102–120. https://doi.org/10.1016/j.jmr.2015.07.001.

(33) Hediger, S.; Lee, D.; Mentink-Vigier, F.; De Paëpe, G. MAS-DNP Enhancements: Hyperpolarization, Depolarization, and Absolute Sensitivity. In *eMagRes*; John Wiley & Sons, Ltd, 2018; pp 105–116. https://doi.org/10.1002/9780470034590.emrstm1559.

(34) Pines, A.; Gibby, M. G.; Waugh, J. S. Proton-enhanced NMR of Dilute Spins in Solids. *The Journal of Chemical Physics* **1973**, *59* (2), 569–590. https://doi.org/10.1063/1.1680061.

(35) Matsuki, Y.; Maly, T.; Ouari, O.; Karoui, H.; Le Moigne, F.; Rizzato, E.; Lyubenova, S.; Herzfeld, J.; Prisner, T.; Tordo, P.; Griffin, R. G. Dynamic Nuclear Polarization with a Rigid Biradical. *Angew. Chem. Int. Ed.* **2009**, *48* (27), 4996–5000. https://doi.org/10.1002/anie.200805940.

(36) Mentink-Vigier, F. Optimizing Nitroxide Biradicals for Cross-Effect MAS-DNP: The Role of g -Tensors' Distance. *Phys. Chem. Chem. Phys.* **2020**, *22* (6), 3643–3652. https://doi.org/10.1039/C9CP06201G.

(37) Perras, F. A.; Sadow, A.; Pruski, M. In Silico Design of DNP Polarizing Agents: Can Current Dinitroxides Be Improved? *ChemPhysChem* **2017**, *18* (16), 2279–2287. https://doi.org/10.1002/cphc.201700299.
(38) Ysacco, C.; Karoui, H.; Casano, G.; Le Moigne, F.; Combes, S.; Rockenbauer, A.; Rosay, M.; Maas, W.; Ouari, O.; Tordo, P. Dinitroxides for Solid State Dynamic Nuclear Polarization. *Appl Magn Reson* **2012**, *43* (1–2), 251–261. https://doi.org/10.1007/s00723-012-0356-3.
(39) Song, C.; Hu, K.-N.; Joo, C.-G.; Swager, T. M.; Griffin, R. G. TOTAPOL: A Biradical Polarizing Agent for Dynamic Nuclear Polarization Experiments in Aqueous Media. *J. Am. Chem. Soc.* **2006**, *128* (35), 11385–11390. https://doi.org/10.1021/ja061284b.
(40) Mentink-Vigier, F.; Marin-Montesinos, I.; Jagtap, A. P.; Halbritter, T.; van Tol, J.; Hediger, S.; Lee, D.; Sigurdsson, S. Th.; De Paëpe, G. Computationally Assisted Design of Polarizing Agents for Dynamic Nuclear Polarization Enhanced NMR: The AsymPol Family. *J. Am. Chem. Soc.* **2018**, *140* (35), 11013–11019. https://doi.org/10.1021/jacs.8b04911.
(41) Harrabi, R.; Halbritter, T.; Aussenac, F.; Dakhlaoui, O.; van Tol, J.; Damodaran, K. K.; Lee, D.; Paul, S.; Hediger, S.; Mentink-Vigier, F.; Sigurdsson, S. Th.; De Paëpe, G. Highly Efficient Polarizing Agents for MAS-DNP of Proton-Dense Molecular Solids. *Angewandte Chemie International Edition* **2022**, *61* (12), e202114103. https://doi.org/10.1002/anie.202114103.
(42) Mathies, G.; Caporini, M. A.; Michaelis, V. K.; Liu, Y.; Hu, K.-N.; Mance, D.; Zweier, J. L.; Rosay, M.; Baldus, M.; Griffin, R. G. Efficient Dynamic Nuclear Polarization at 800 MHz/527 GHz with Trityl-Nitroxide Biradicals. *Angew. Chem.* **2015**, *127* (40), 11936–11940. https://doi.org/10.1002/ange.201504292.
(43) Equbal, A.; Tagami, K.; Han, S. Balancing Dipolar and Exchange Coupling in Biradicals to Maximize Cross Effect Dynamic Nuclear Polarization. *Phys. Chem. Chem. Phys.* **2020**, *22* (24), 13569–13579. https://doi.org/10.1039/D0CP02051F.
(44) Mentink-Vigier, F.; Mathies, G.; Liu, Y.; Barra, A.-L.; Caporini, M. A.; Lee, D.; Hediger, S.; G. Griffin, R.; De Paëpe, G. Efficient Cross-Effect Dynamic Nuclear Polarization without Depolarization in High-Resolution MAS NMR. *Chem. Sci.* **2017**, *8* (12), 8150–8163. https://doi.org/10.1039/C7SC02199B.
(45) Zagdoun, A.; Casano, G.; Ouari, O.; Lapadula, G.; Rossini, A. J.; Lelli, M.; Baffert, M.; Gajan, D.; Veyre, L.; Maas, W. E.; Rosay, M.; Weber, R. T.; Thieuleux, C.; Coperet, C.; Lesage, A.; Tordo, P.; Emsley, L. A Slowly Relaxing Rigid Biradical for Efficient Dynamic Nuclear Polarization Surface-Enhanced NMR Spectroscopy: Expeditious Characterization of Functional Group Manipulation in Hybrid Materials. *J. Am. Chem. Soc.* **2012**, *134* (4), 2284–2291. https://doi.org/10.1021/ja210177v.
(46) Sauvée, C.; Casano, G.; Abel, S.; Rockenbauer, A.; Akhmetzyanov, D.; Karoui, H.; Siri, D.; Aussenac, F.; Maas, W.; Weber, R. T.; Prisner, T.; Rosay, M.; Tordo, P.; Ouari, O. Tailoring of Polarizing Agents in the bTurea Series for Cross-Effect Dynamic Nuclear

Polarization in Aqueous Media. *Chem. Eur. J.* **2016**, *22* (16), 5598–5606. https://doi.org/10.1002/chem.201504693.

(47) Kubicki, D. J.; Casano, G.; Schwarzwälder, M.; Abel, S.; Sauvée, C.; Ganesan, K.; Yulikov, M.; Rossini, A. J.; Jeschke, G.; Copéret, C.; Lesage, A.; Tordo, P.; Ouari, O.; Emsley, L. Rational Design of Dinitroxide Biradicals for Efficient Cross-Effect Dynamic Nuclear Polarization. *Chem. Sci.* **2016**, *7* (1), 550–558. https://doi.org/10.1039/C5SC02921J.

(48) Jagtap, A. P.; Geiger, M.-A.; Stöppler, D.; Orwick-Rydmark, M.; Oschkinat, H.; Sigurdsson, S. Th. bcTol: A Highly Water-Soluble Biradical for Efficient Dynamic Nuclear Polarization of Biomolecules. *Chem. Commun.* **2016**, *52* (43), 7020–7023. https://doi.org/10.1039/C6CC01813K.

(49) Geiger, M. A.; Jagtap, A. P.; Kaushik, M.; Sun, H.; Stöppler, D.; Sigurdsson, S. T.; Corzilius, B.; Oschkinat, H. Efficiency of Water-Soluble Nitroxide Biradicals for Dynamic Nuclear Polarization in Rotating Solids at 9.4 T: bcTol-M and Cyolyl-TOTAPOL as New Polarizing Agents. *Chemistry - A European Journal* **2018**, *24* (51), 13485–13494. https://doi.org/10.1002/chem.201801251.

(50) Venkatesh, A.; Casano, G.; Rao, Y.; De Biasi, F.; Perras, F. A.; Kubicki, D. J.; Siri, D.; Abel, S.; Karoui, H.; Yulikov, M.; Ouari, O.; Emsley, L. Deuterated TEKPol Biradicals and the Spin-Diffusion Barrier in MAS DNP. *Angew Chem Int Ed* **2023**, *62* (31), e202304844. https://doi.org/10.1002/anie.202304844.

(51) Mentink-Vigier, F.; Paul, S.; Lee, D.; Feintuch, A.; Hediger, S.; Vega, S.; De Paëpe, G. Nuclear Depolarization and Absolute Sensitivity in Magic-Angle Spinning Cross Effect Dynamic Nuclear Polarization. *Phys. Chem. Chem. Phys.* **2015**, *17* (34), 21824–21836. https://doi.org/10.1039/C5CP03457D.

(52) Thurber, K. R.; Tycko, R. Perturbation of Nuclear Spin Polarizations in Solid State NMR of Nitroxide-Doped Samples by Magic-Angle Spinning without Microwaves. *The Journal of Chemical Physics* **2014**, *140* (18), 184201. https://doi.org/10.1063/1.4874341.

(53) Mentink-Vigier, F.; Vega, S.; De Paepe, G. Fast and Accurate MAS–DNP Simulations of Large Spin Ensembles. *Physical Chemistry Chemical Physics* **2017**, *19* (5), 3506–3522. https://doi.org/10.1039/C6CP07881H.

(54) Ernst, M.; Meier, B. H. Spin Diffusion in Solids. In *Studies in Physical and Theoretical Chemistry*; Elsevier, 1998; Vol. 84, pp 83–121. https://doi.org/10.1016/S0167-6881(98)80007-4.

(55) van der Wel, P. C. A.; Hu, K.-N.; Lewandowski, J.; Griffin, R. G. Dynamic Nuclear Polarization of Amyloidogenic Peptide Nanocrystals: GNNQQNY, a Core Segment of the Yeast Prion Protein Sup35p. *J. Am. Chem. Soc.* **2006**, *128* (33), 10840–10846. https://doi.org/10.1021/ja0626685.

(56) Rossini, A. J.; Zagdoun, A.; Hegner, F.; Schwarzwälder, M.; Gajan, D.; Copéret, C.; Lesage, A.; Emsley, L. Dynamic Nuclear Polarization NMR Spectroscopy of Microcrystalline Solids. *J. Am. Chem. Soc.* **2012**, *134* (40), 16899–16908. https://doi.org/10.1021/ja308135r.

(57) Prisco, N. A.; Pinon, A. C.; Emsley, L.; Chmelka, B. F. Scaling Analyses for Hyperpolarization Transfer across a Spin-Diffusion Barrier and into Bulk Solid Media. *Phys. Chem. Chem. Phys.* **2021**, *23* (2), 1006–1020. https://doi.org/10.1039/D0CP03195J.
(58) Stern, Q.; Cousin, S. F.; Mentink-Vigier, F.; Pinon, A. C.; Elliott, S. J.; Cala, O.; Jannin, S. Direct Observation of Hyperpolarization Breaking through the Spin Diffusion Barrier. *Science Advances* **2021**, *7* (18), eabf5735. https://doi.org/10.1126/sciadv.abf5735.
(59) Wolfe, J. P. Direct Observation of a Nuclear Spin Diffusion Barrier. *Phys. Rev. Lett.* **1973**, *31* (15), 907–910. https://doi.org/10.1103/PhysRevLett.31.907.
(60) Smith, A. A.; Corzilius, B.; Barnes, A. B.; Maly, T.; Griffin, R. G. Solid Effect Dynamic Nuclear Polarization and Polarization Pathways. *The Journal of Chemical Physics* **2012**, *136* (1), 015101. https://doi.org/10.1063/1.3670019.
(61) Mentink-Vigier, F.; Barra, A.-L.; van Tol, J.; Hediger, S.; Lee, D.; De Paepe, G. De Novo Prediction of Cross-Effect Efficiency for Magic Angle Spinning Dynamic Nuclear Polarization. *Physical Chemistry Chemical Physics* **2019**, *21* (4), 2166–2176. https://doi.org/10.1039/C8CP06819D.
(62) Perras, F. A.; Raju, M.; Carnahan, S. L.; Akbarian, D.; van Duin, A. C. T.; Rossini, A. J.; Pruski, M. Full-Scale Ab Initio Simulation of Magic-Angle-Spinning Dynamic Nuclear Polarization. *J. Phys. Chem. Lett.* **2020**, *11* (14), 5655–5660. https://doi.org/10.1021/acs.jpclett.0c00955.
(63) Mentink-Vigier, F.; Dubroca, T.; Van Tol, J.; Sigurdsson, S. Th. The Distance between G-Tensors of Nitroxide Biradicals Governs MAS-DNP Performance: The Case of the bTurea Family. *Journal of Magnetic Resonance* **2021**, *329*, 107026. https://doi.org/10.1016/j.jmr.2021.107026.
(64) Perras, F. A.; Pruski, M. Large-Scale *Ab Initio* Simulations of MAS DNP Enhancements Using a Monte Carlo Optimization Strategy. *The Journal of Chemical Physics* **2018**, *149* (15), 154202. https://doi.org/10.1063/1.5042651.
(65) Gafurov, M.; Lyubenova, S.; Denysenkov, V.; Ouari, O.; Karoui, H.; Le Moigne, F.; Tordo, P.; Prisner, T. EPR Characterization of a Rigid Bis-TEMPO–Bis-Ketal for Dynamic Nuclear Polarization. *Appl Magn Reson* **2010**, *37* (1–4), 505–514. https://doi.org/10.1007/s00723-009-0069-4.
(66) Zagdoun, A.; Casano, G.; Ouari, O.; Schwarzwälder, M.; Rossini, A. J.; Aussenac, F.; Yulikov, M.; Jeschke, G.; Copéret, C.; Lesage, A.; Tordo, P.; Emsley, L. Large Molecular Weight Nitroxide Biradicals Providing Efficient Dynamic Nuclear Polarization at Temperatures up to 200 K. *J. Am. Chem. Soc.* **2013**, *135* (34), 12790–12797. https://doi.org/10.1021/ja405813t.
(67) Geiger, M. A.; Orwick-Rydmark, M.; Märker, K.; Franks, W. T.; Akhmetzyanov, D.; Stöppler, D.; Zinke, M.; Specker, E.; Nazaré, M.; Diehl, A.; van Rossum, B.-J.; Aussenac, F.; Prisner, T. F.; Akbey, U.; Oschkinat, H. Temperature Dependence of Cross-Effect Dynamic Nuclear Polarization in Rotating Solids: Advantages of Elevated Temperatures. *Phys. Chem. Chem. Phys.* **2016**, *18* (44), 30696–30704. https://doi.org/10.1039/C6CP06154K.

(68) Perras, F. A.; Reinig, R. R.; Slowing, I. I.; Sadow, A. D.; Pruski, M. Effects of Biradical Deuteration on the Performance of DNP: Towards Better Performing Polarizing Agents. *Phys. Chem. Chem. Phys.* **2016**, *18* (1), 65–69. https://doi.org/10.1039/C5CP06505D.
(69) Sauvée, C.; Rosay, M.; Casano, G.; Aussenac, F.; Weber, R. T.; Ouari, O.; Tordo, P. Highly Efficient, Water-Soluble Polarizing Agents for Dynamic Nuclear Polarization at High Frequency. *Angew. Chem. Int. Ed.* **2013**, *52* (41), 10858–10861. https://doi.org/10.1002/anie.201304657.
(70) Becker-Baldus, J.; Yeliseev, A.; Joseph, T. T.; Sigurdsson, S. Th.; Zoubak, L.; Hines, K.; Iyer, M. R.; van den Berg, A.; Stepnowski, S.; Zmuda, J.; Gawrisch, K.; Glaubitz, C. Probing the Conformational Space of the Cannabinoid Receptor 2 and a Systematic Investigation of DNP-Enhanced MAS NMR Spectroscopy of Proteins in Detergent Micelles. *ACS Omega* **2023**, *8* (36), 32963–32976. https://doi.org/10.1021/acsomega.3c04681.
(71) Lund, A.; Casano, G.; Menzildjian, G.; Kaushik, M.; Stevanato, G.; Yulikov, M.; Jabbour, R.; Wisser, D.; Renom-Carrasco, M.; Thieuleux, C.; Bernada, F.; Karoui, H.; Siri, D.; Rosay, M.; Sergeyev, I. V.; Gajan, D.; Lelli, M.; Emsley, L.; Ouari, O.; Lesage, A. TinyPols: A Family of Water-Soluble Binitroxides Tailored for Dynamic Nuclear Polarization Enhanced NMR Spectroscopy at 18.8 and 21.1 T. *Chem. Sci.* **2020**, *11* (10), 2810–2818. https://doi.org/10.1039/C9SC05384K.
(72) Chaudhari, S. R.; Berruyer, P.; Gajan, D.; Reiter, C.; Engelke, F.; Silverio, D. L.; Copéret, C.; Lelli, M.; Lesage, A.; Emsley, L. Dynamic Nuclear Polarization at 40 kHz Magic Angle Spinning. *Phys. Chem. Chem. Phys.* **2016**, *18* (15), 10616–10622. https://doi.org/10.1039/C6CP00839A.
(73) Soetbeer, J.; Gast, P.; Walish, J. J.; Zhao, Y.; George, C.; Yang, C.; Swager, T. M.; Griffin, R. G.; Mathies, G. Conformation of Bis-Nitroxide Polarizing Agents by Multi-Frequency EPR Spectroscopy. *Phys. Chem. Chem. Phys.* **2018**, *20* (39), 25506–25517. https://doi.org/10.1039/C8CP05236K.
(74) Perras, F. A.; Carnahan, S. L.; Lo, W.-S.; Ward, C. J.; Yu, J.; Huang, W.; Rossini, A. J. Hybrid Quantum-Classical Simulations of Magic Angle Spinning Dynamic Nuclear Polarization in Very Large Spin Systems. *J. Chem. Phys.* **2022**, *156* (12), 124112. https://doi.org/10.1063/5.0086530.
(75) Wisser, D.; Karthikeyan, G.; Lund, A.; Casano, G.; Karoui, H.; Yulikov, M.; Menzildjian, G.; Pinon, A. C.; Purea, A.; Engelke, F.; Chaudhari, S. R.; Kubicki, D.; Rossini, A. J.; Moroz, I. B.; Gajan, D.; Copéret, C.; Jeschke, G.; Lelli, M.; Emsley, L.; Lesage, A.; Ouari, O. BDPA-Nitroxide Biradicals Tailored for Efficient Dynamic Nuclear Polarization Enhanced Solid-State NMR at Magnetic Fields up to 21.1 T. *J. Am. Chem. Soc.* **2018**, *140* (41), 13340–13349. https://doi.org/10.1021/jacs.8b08081.
(76) Halbritter, T.; Harrabi, R.; Paul, S.; Van Tol, J.; Lee, D.; Hediger, S.; Sigurdsson, S. Th.; Mentink-Vigier, F.; De Paëpe, G. PyrroTriPol: A Semi-Rigid Trityl-Nitroxide for High Field Dynamic Nuclear Polarization. *Chem. Sci.* **2023**, *14* (14), 3852–3864. https://doi.org/10.1039/D2SC05880D.

(77) Javed, A.; Equbal, A. Direct Sensing of Remote Nuclei: Expanding the Reach of Cross-Effect Dynamic Nuclear Polarization. arXiv September 27, 2023. https://doi.org/10.48550/arXiv.2309.15653.